Potential of antiviral drug oseltamivir for the treatment of liver cancer

PEI-JU HUANG[1], CHUN-CHING CHIU[2], MIN-HUA HSIAO[3], JIA LE YOW[3,4], BOR-SHOW TZANG[3-6] and TSAI-CHING HSU[3,5,6]

[1]Department of Family Medicine, Changhua Christian Hospital; [2]Department of Neurology and Department of Medical Intensive Care Unit, Changhua Christian Hospital, Changhua 500; [3]Institute of Medicine, College of Medicine, Chung Shan Medical University; [4]Department of Biochemistry, School of Medicine, Chung Shan Medical University; [5]Immunology Research Center, Chung Shan Medical University; [6]Department of Medical Research, Chung Shan Medical University Hospital, Taichung 402, Taiwan, R.O.C.

Received August 13, 2021; Accepted October 26, 2021

DOI: 10.3892/ijo.2021.5289

Abstract. Liver cancer is a leading cause of cancer-related mortality globally. Since hepatitis virus infections have been strongly associated with the incidence of liver cancer, studies concerning the effects of antiviral drugs on liver cancer have attracted great attention in recent years. The present study investigated the effects of two anti-hepatitis virus drugs, lamivudine and ribavirin, and one anti-influenza virus drug, oseltamivir, on liver cancer cells to assess alternative methods for treating liver cancer. MTT assays, wound healing assays, Transwell assays, flow cytometry, immunoblotting, ELISA, immunofluorescence staining and a xenograft animal model were adopted to verify the effects of lamivudine, ribavirin and oseltamivir on liver cancer cells. Treatment with ribavirin and oseltamivir for 24 and 48 h significantly decreased the viability of both Huh-7 and HepG2 cells compared with that of THLE-3 cells in a dose-dependent manner. The subsequent investigations focused on oseltamivir, considering the more serious clinical adverse effects of ribavirin than those of oseltamivir. Significantly decreased migration and invasion were observed in both Huh-7 and HepG2 cells that were treated with oseltamivir for 24 and 48 h. In addition, oseltamivir significantly increased autophagy in Huh-7 cells, as revealed by the significantly higher ratios of LC3-II/LC3-I, increased expression of Beclin-1, and decreased expression of p62, whereas no significant increases in the expression of apoptosis-related proteins, including Apaf-1, cleaved caspase-3, and cleaved PARP-1, were detected. Notably, apoptosis and autophagy were significantly increased in HepG2 cells in the presence of oseltamivir, as revealed by the significant increases in the expression of Apaf-1, cleaved caspase-3, and cleaved PARP-1, the higher ratios of LC3-II/LC3-I, the increased expression of Beclin-1, and the decreased expression of p62. Additionally, significant inhibitory effects of oseltamivir on xenografted Huh-7 cells in athymic nude mice were observed. The present study, for the first time to the best of our knowledge, reported the differential effects of oseltamivir on inducing liver cancer cell death both *in vitro* and *in vivo* and may provide an alternative approach for treating liver cancer.

Correspondence to: Dr Bor-Show Tzang, Department of Biochemistry, School of Medicine, Chung Shan Medical University, 110 Sec. 1, Jianguo N. Road, Taichung 402, Taiwan, R.O.C.
E-mail: bstzang@csmu.edu.tw

Dr Tsai-Ching Hsu, Institute of Medicine, College of Medicine, Chung Shan Medical University, 110 Sec. 1, Jianguo N. Road, Taichung 402, Taiwan, R.O.C.
E-mail: htc@csmu.edu.tw

Key words: liver cancer, oseltamivir, autophagy

Introduction

Evidence has indicated that more than 850,000 patients are diagnosed with liver cancer each year worldwide, indicating that liver cancer is a major health issue. Hepatocellular carcinoma (HCC) accounts for approximately 90% of all primary liver cancer cases and is known as the second leading cause of cancer-related deaths worldwide (1,2). Notably, investigations have revealed that the age-standardized incidence rates (ASIRs) of liver cancer in eastern Asia are higher than those in other countries worldwide. In Taiwan, liver cancer was among the top four most common cancers in 2014, and the ASIR has decreased over the past several years (3). The development of liver cancer has been linked to a variety of risk factors, including sex, ethnicity, chronic viral hepatitis, cirrhosis, inherited metabolic disorders, alcohol abuse, tobacco use, aflatoxins, obesity, and type-2 diabetes (4,5).

The incidence of primary liver cancer is largely explained by infection with hepatitis B and C viruses, and such infections account for over 80% of liver cancer cases worldwide (6). In fact, numerous studies have demonstrated a strong correlation between chronic viral hepatitis, particularly hepatitis induced by hepatitis B and C viruses and liver cancer development (6-9).

A previous study using an algorithm reported that patients who met the criteria for chronic hepatitis B virus (HBV) infection had a significantly higher incidence, ranging from 30 to 140 times, of developing HCC compared with patients without HBV (10). Another cohort study also indicated that hepatitis C virus (HCV) infection was associated with the highest incidence of HCC in patients with cirrhosis, particularly in Japan (11). More than half of HCC cases worldwide are attributable to HBV infection. Case-control and cohort studies reported that the relative risk of HCC in patients with HBV infection ranges from 5 to 49 and from 7 to 98, respectively (12,13).

Evidence has indicated that chronic HBV or HCV infection may cause liver cirrhosis, which is also the most important risk factor for liver cancer. Various studies have reported that sustained reduction in HBV/HCV replication lowers the risk of HCC in patients with HBV/HCV-associated cirrhosis (7,11). Accordingly, the primary strategy for liver cancer prevention is the elimination of viral infection by antiviral therapy (14,15). However, information concerning the anti-liver cancer effects of antiviral drugs remains obscure. Therefore, the present study investigated the effects of two anti-hepatitis virus drugs, lamivudine and ribavirin, and one anti-influenza virus drug, oseltamivir, on liver cancer cells to identify alternative methods for the treatment of liver cancer.

Materials and methods

Cell culture. Normal human liver epithelial cell line THLE-3 [CRL-11233; American Type Culture Collection (ATCC)] and two liver cancer cell lines, Huh-7 (JCRB0403; JCRB Cell Bank) and C3A [HepG2/C3A, derivative of HepG2 (ATCC HB-8065)] (CRL-10741; ATCC) were maintained following the manufacturers' instructions in bronchial epithelial cell growth medium (BEGM) (Lonza Group, Ltd.) or Dulbecco's modified Eagle's medium (DMEM) supplemented with 10% fetal bovine serum (FBS; Gibco; Thermo Fisher Scientific, Inc.), respectively. The cell lines used in the present study were subjected to short tandem repeat (STR) profiling through the National Cheng Kung University (NCKU) Center for Genomic Medicine to confirm their authenticity. The antiviral drugs, including lamivudine (Zeffix Tablet 100 mg; GlaxoSmithKline), ribavirin (Robatrol capsule 200 mg) and oseltamivir (Tamiflu capsule 75 mg; both from Roche Diagnostics) were obtained from Changhua Christian Hospital, Taiwan.

Cell viability. To determine the survival of cells, a 3-(4,5-dimethylthiazol-2-yl)-2,5-diphenyl tetrazolium bromide (MTT) assay was performed. A total of $1x10^5$ cells were cultured overnight at 37˚C in each well of a 24-well plate in a cell incubator. Following incubation with different concentrations of antiviral drugs (lamivudine and ribavirin: 0, 1,000, 2,000, 3,000, 4,000 and 5,000 μM; oseltamivir: 0, 50, 100, 250, 500 and 1,000 μM), the culture medium was removed and MTT reagent (0.5 mg/ml) was added to each well and incubated for another 4 h. A total of 0.3 ml dimethyl sulfoxide (DMSO) was then added to each well of the plate and the absorbance was measured at 570 nm with a microplate reader (SpectraMax M5; Molecular Devices, LLC).

Wound healing assay. To verify the effects of oseltamivir on migration of liver cancer cells, a wound healing assay was performed. Briefly, Huh-7 and HepG2 cells were cultured in serum-free DMEM medium overnight in a 6-well plate ($5x10^6$ cells/well) until reaching 90% confluency. A sterilized 200-μl pipette tip was used to make a wound by scratching across the well surface. Following washing out the debris with fresh medium, the cells were incubated at 37˚C for 24 and 48 h in the presence of various concentrations (0, 50, 100, 250, 500 and 1,000 μM) of oseltamivir and images of the wound gaps were captured at 0, 24 and 48 h using Zeiss AxioVert 200 inverted fluorescence microscope. The cell-migrated areas were calculated with Motic Images 2.0 software (Motic Incoporation, Ltd.).

Transwell migration and invasion assays. To verify the effects of oseltamivir on hepatoma cell migration and invasion, 24-well Millicell Hanging Cell Culture inserts (8-μm pore size; EMD Millipore) were used. For the invasion assay, the upper chambers were precoated with 0.4 mg/ml Matrigel (BD Biosciences) at 37˚C for 24 h. Briefly, the upper chamber containing serum-free DMEM medium ($2x10^5$ cells) and various concentrations (0, 50, 100, 250, 500 and 1,000 μM) of oseltamivir, and the bottom chamber containing standard medium (DMEM with 10% FBS) was combined and incubated at 37˚C for 24 and 48 h in a cell incubator. Next, the migrating cells were fixed with neutral-buffered formalin (10%) at 25˚C for 2 h and then stained with 0.05% Giemsa stain at 25˚C for 2 h. A total of six random fields were counted for each experiment under a light microscope at a magnification of x200 per filter.

Flow cytometry. For flow cytometric analysis, the cells were incubated with various concentrations of oseltamivir (0, 50, 100, 250, 500 and 1,000 μM) at 37˚C for 24 and 48 h. Following incubation, the $1x10^6$ cells were harvested, washed with phosphate-buffered saline (PBS), and fixed with 70% alcohol for 16 h at -20˚C. The cells were then washed with PBS and transferred into 12x75-mm tubes. A total of 10 μl of propidium iodide (PI) staining solution was added and chilled on ice in the dark. Following filtration through a 40-μm nylon screen, the cells were analyzed with a FACSCalibur analyzer (Nippon Becton Dickinson) and data analysis was performed using WinMDI 2.9 (The Scripps Research Institute, San Diego, USA).

Protein preparation and immunoblotting. The cell pellets were collected by centrifugation at 800 x g for 5 min at 4˚C and suspended in 600 μl PRO-PREP™ buffer (iNtRON Biotechnology, Inc.) for lysis. The supernatant was then obtained by centrifugation at 16,600 x g for 5 min at 4˚C. The concentrations of protein were measured by a modified Bradford's assay using a spectrophotometer (Hitachi U 3000; HITACHI) at 595 nm with BSA (Sigma-Aldrich; Merck KGaA) as the standard. For immunoblotting, extracted proteins (25 μg/lane) were separated by 8-12% SDS-PAGE and electrophoretically transferred to PVDF membranes (Immobilon-E, 0.45 μM; MilliporeSigma). After blocking in 5% non-fat dry milk for 1 h at 25˚C, the membranes were incubated with antibodies against Apaf-1 (1:2,000; product code ab2000; Abcam), cleaved

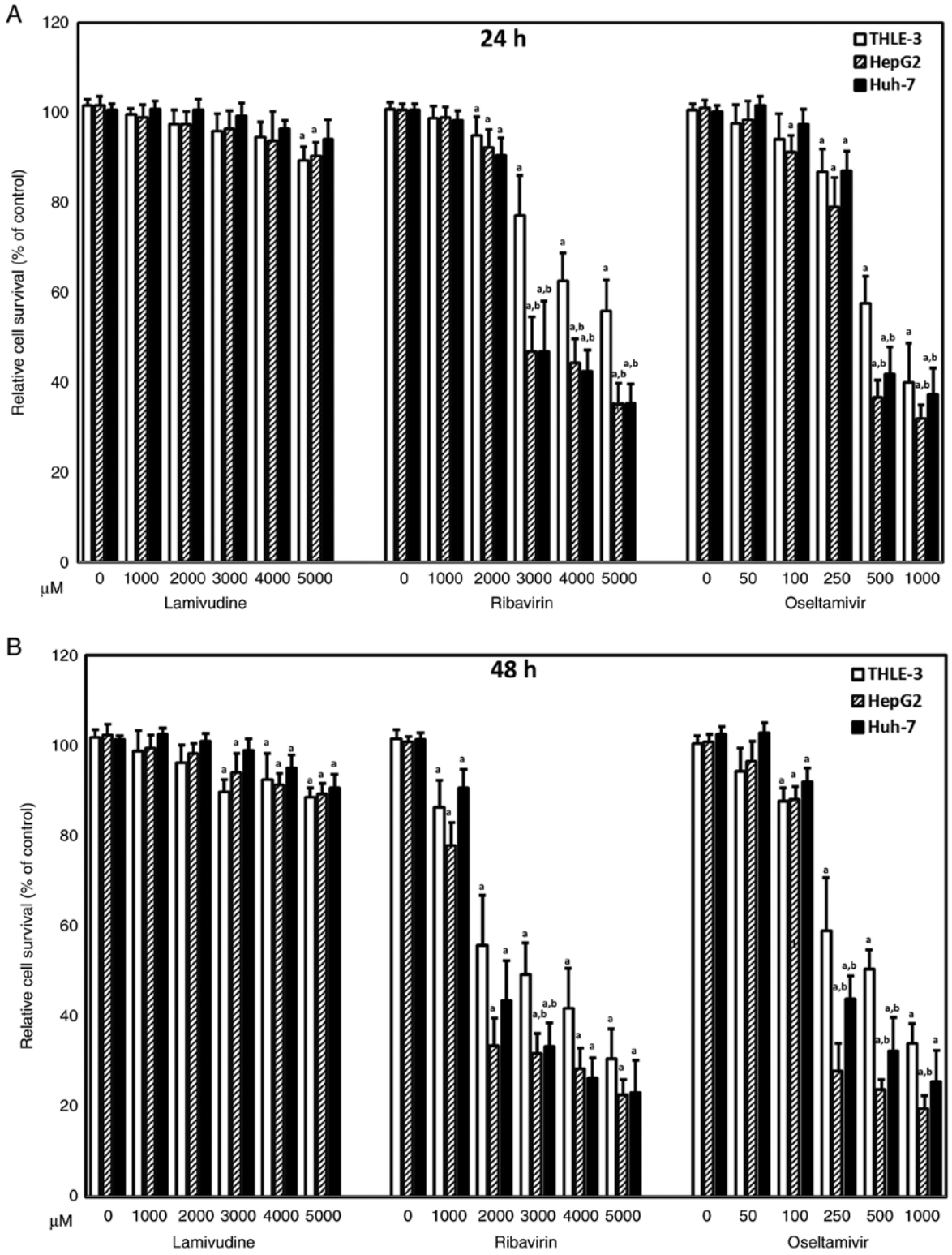

Figure 1. Relative cell survival of THLE-3, Huh-7 and HepG2 cells. Survival ratio of THLE-3, Huh-7 and HepG2 cells in the presence of various concentrations of lamivudine, ribavirin and oseltamivir antiviral drugs for (A) 24 and (B) 48 h. At least three-repeated tests were performed. [a]P<0.05 compared with the control (0 μM); and [b]P<0.05 compared with THLE-3 cells.

caspase-3 (1:500; product no. AB3623; Sigma-Aldrich; Merck KGaA), cleaved PARP-1 (1:500; cat. no. sc-7150; Santa Cruz Biotechnology, Inc.), LC3 (1:5,000; cat. no. NB100-2220), Beclin-1 (1:10,000; cat. no. NB110-87318), and p62/SQSTM1 (1:4,000; cat. no. NBP1-48320; all from Novus Biologicals, LLC) and β-actin (1:5,000; cat. no. MAB1501; EMD Millipore) were used to detect apoptosis and autophagy. Briefly, the PVDF membranes (Immobilon-E, 0.45 μM; MilliporeSigma) were incubated with the antibodies for 3 h at 25˚C. Next, the secondary antibodies conjugated with horseradish peroxidase (HRP) (1:5,000; cat. no. sc-2004 or sc-2005; Santa Cruz Biotechnology, Inc.) were added and incubated

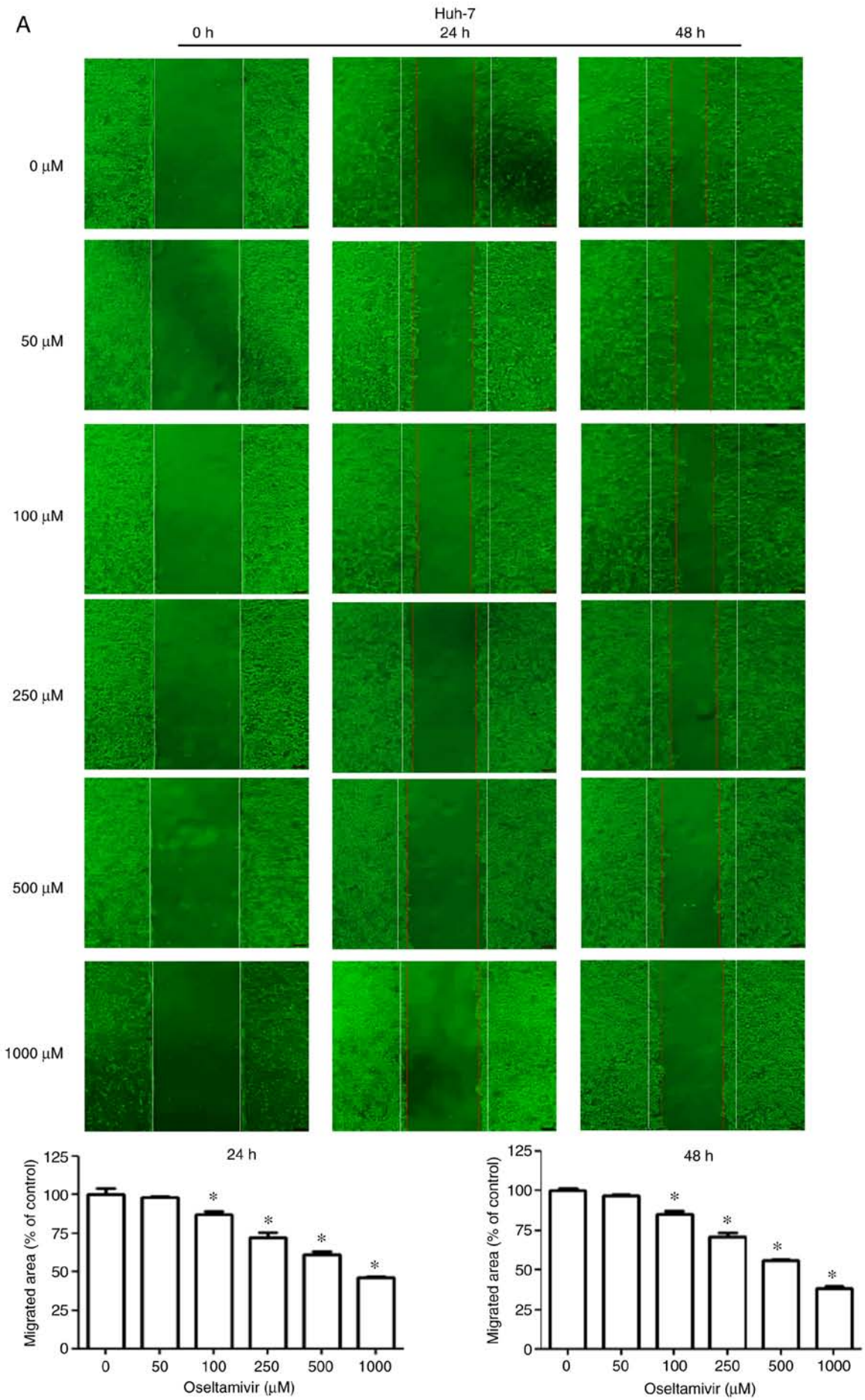

Figure 2. Continued.

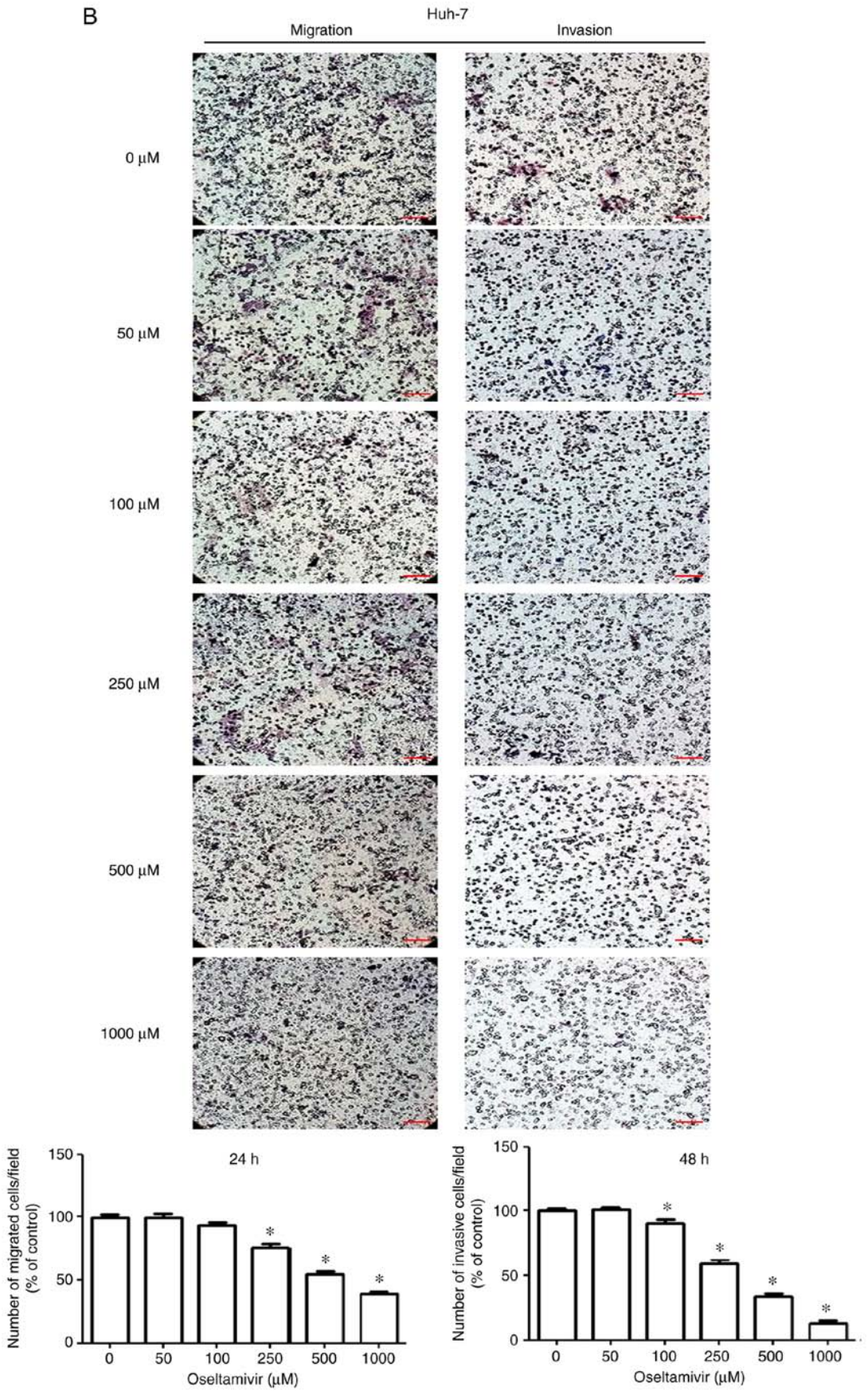

Figure 2. Effects of oseltamivir on the migration and invasion in Huh-7 cells. Wound healing experiments and Transwell assays were used to examine the wound healing capacity (magnification, x50), migration (magnification, x200) and invasion (magnification, x200) of Huh-7 cells. (A) Representative images of Huh-7 cells treated with oseltamivir for 0, 24, and 48 h following wounding. The migrated areas were calculated (Motic Images 2.0 software) and the percentage of wound closure was presented relative to the control (0 μM). (B) Representative images of migrated and invading Huh-7 cells treated with oseltamivir for 24 h. Percentage of migrated and invading cells was shown relative to the control (0 μM). At least three-repeated tests were performed. Scale bars, 20 μm. *P<0.05 compared with control (0 μM).

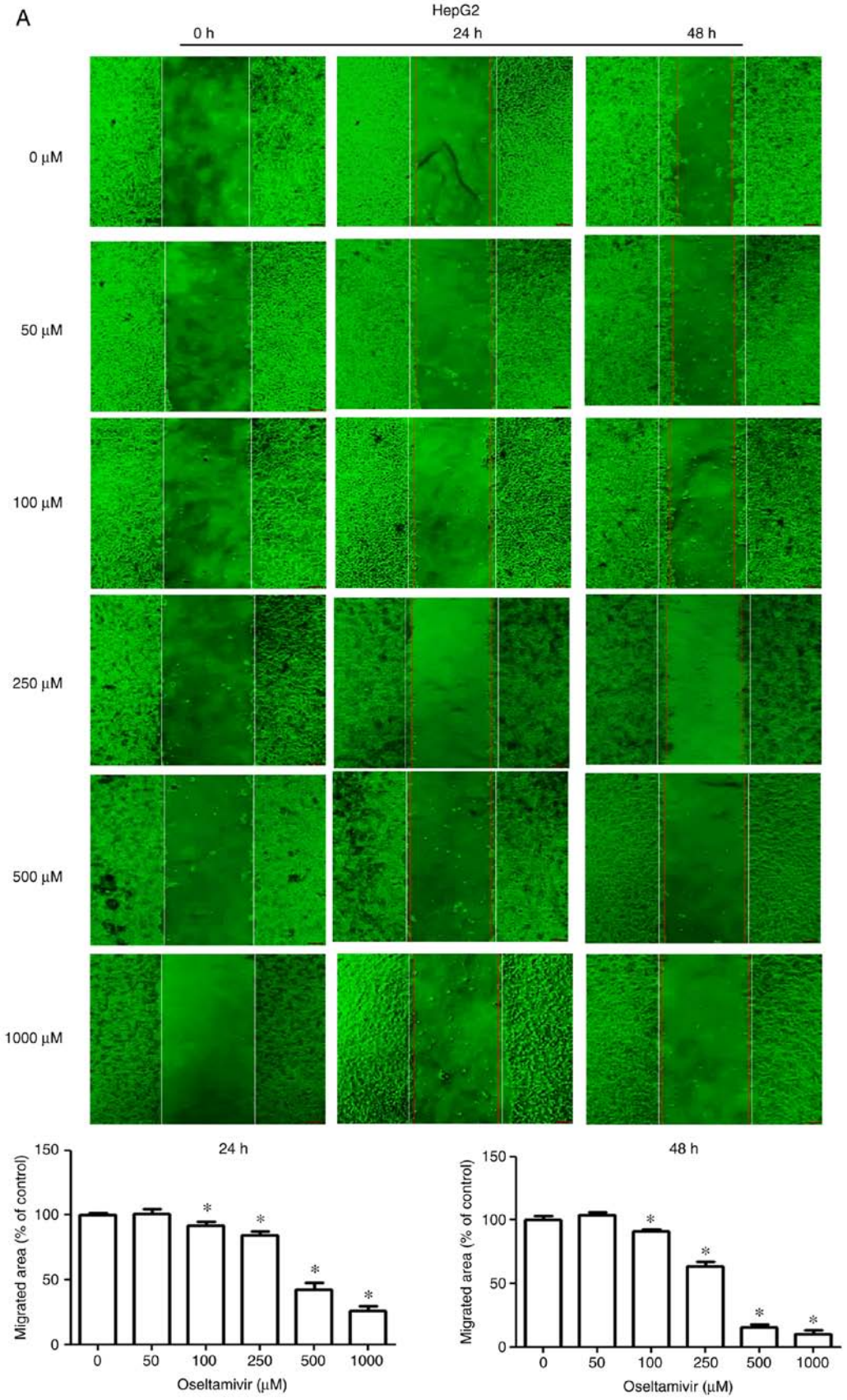

Figure 3. Continued.

for 1 h at 25˚C. To detect the antigen-antibody complexes, Immobilion Western HRP Chemiluminescent Substrate (EMD Millipore) and a densitometry apparatus LAS-4000 (Image Analysis Software: GE ImageQuant TL 8.1; GE Healthcare Life Sciences) were used. In addition, an autophagy inhibitor, chloroquine diphosphate (CQ; cat. no. L10382;

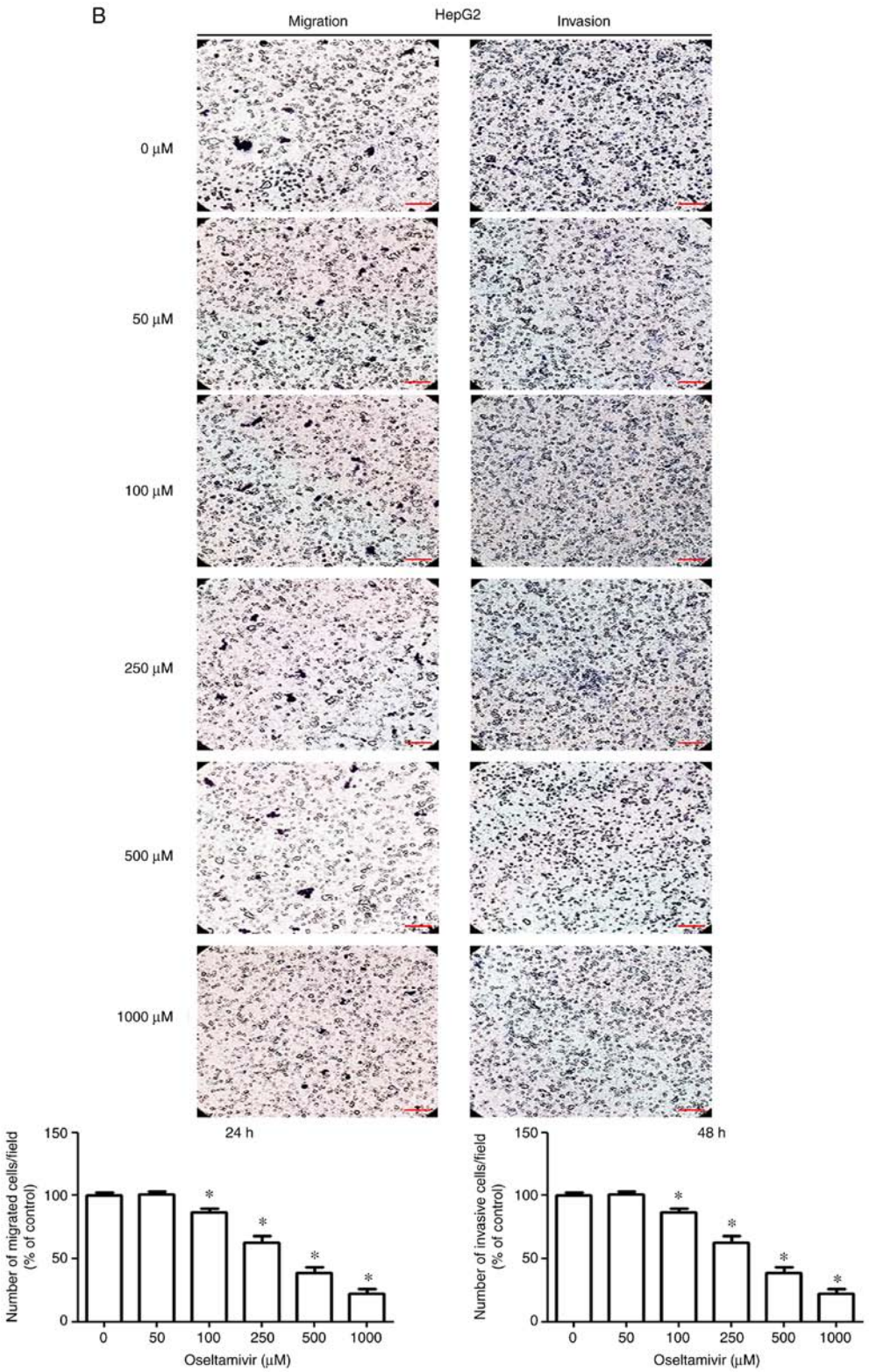

Figure 3. Effects of oseltamivir on the migration and invasion in HepG2 cells. Wound healing experiments and Transwell assays were used to examine the wound healing capacity (magnification, x50), migration (magnification, x200) and invasion (magnification, x200) of HepG2 cells. (A) Representative images of HepG2 cells treated with oseltamivir for 0, 24, and 48 h following wounding. The migrated areas were calculated (Motic Images 2.0 software) and the percentage of wound closure was presented relative to the control (0 μM). (B) Representative images of migrated and invading HepG2 cells treated with oseltamivir for 24 h. Percentage of migrated and invading cells was shown relative to the control (0 μM). At least three-repeated tests were performed. Scale bars, 20 μm. *P<0.05 compared with control (0 μM).

LC3B Antibody Kit; Invitrogen; Thermo Fisher Scientific Inc.), was used to verify the participation of the autophagic mechanism to oseltamivir-induced death in Huh-7 and HepG2 cells. Following pre-treatment of Huh-7 and HepG2 cells with CQ (25 μM) for 1 h, the cells were then incubated with 1 mM oseltamivir for 24 h at 37˚C.

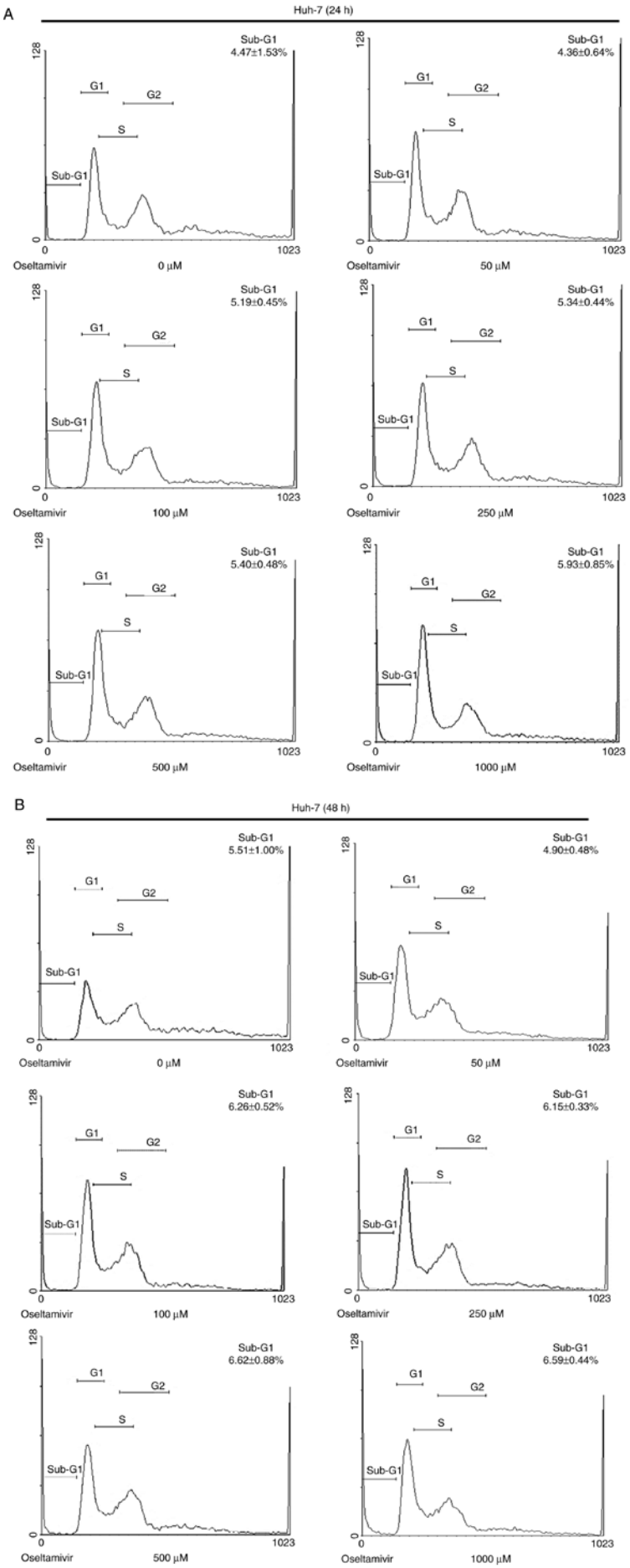

Figure 4. Continued.

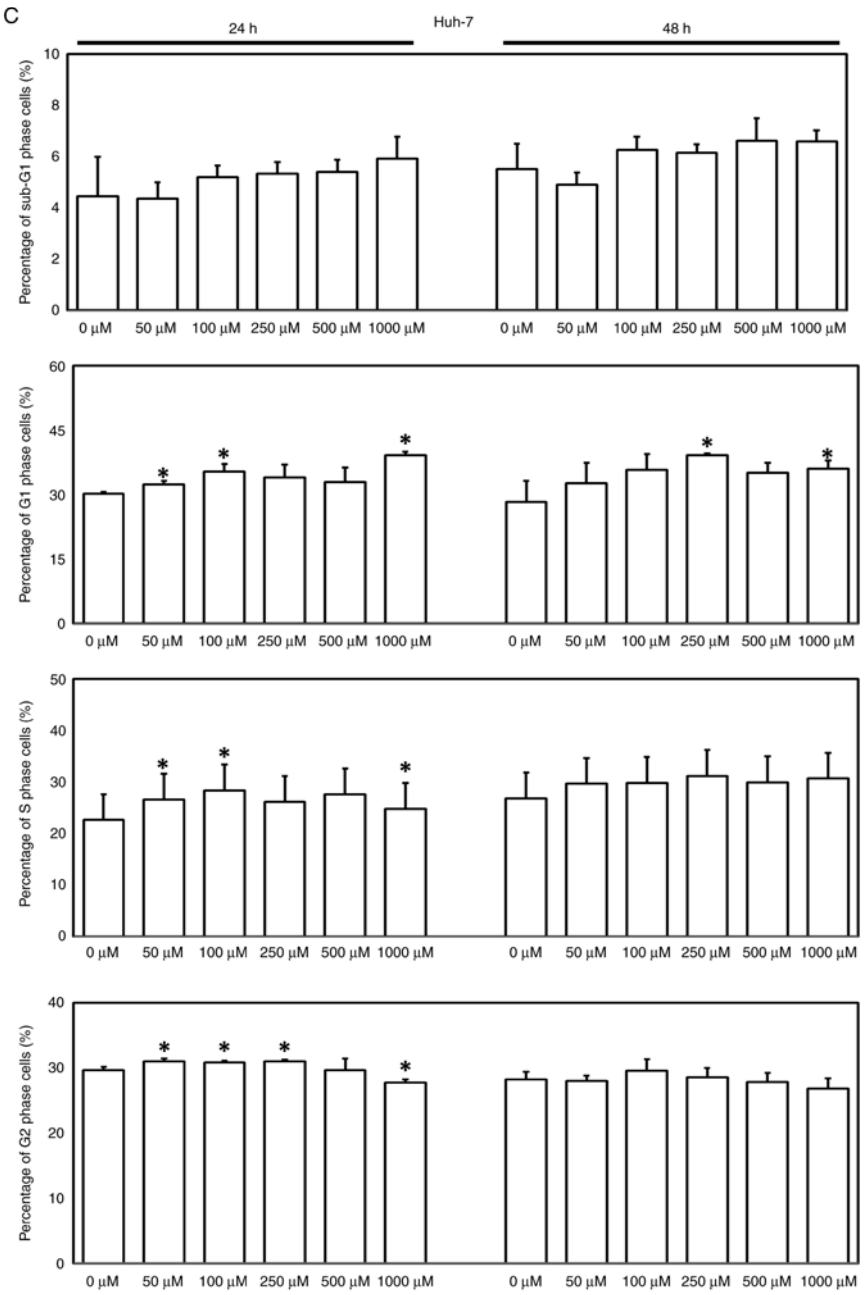

Figure 4. Effects of oseltamivir on the cell cycle in Huh-7 cells. Representative results of the flow cytometric analysis of Huh-7 cells in the presence of oseltamivir for (A) 24 h and (B) 48 h. (C) Bar diagram demonstrating the percentage of sub-G1, G1, S and G2 proportion in Huh-7 cells. At least three-repeated tests were performed. *P<0.05 compared with control (0 μM).

Enzyme-linked immunosorbent assay (ELISA). An active caspase-3 ELISA Kit (Human active caspase-3 (Ser29) SimpleStep ELISA kit; product code ab181418; Abcam) was used to measure active caspase-3 according to the manufacturer's protocol.

Immunofluorescence staining. An LC3B Antibody kit (cat. no. L10382; Invitrogen; Thermo Fisher Scientific Inc.) was used for autophagy detection according to the manufacturer's protocol. Briefly, the $1x10^6$ cells were seeded on Millicell EZ SLIDE 8-well glass slides and maintained with fresh DMEM with 10% FBS medium containing various doses of oseltamivir (0, 50, 100, 250, 500 and 1,000 μM) for 24 h. Next, the cells were blocked in 2% BSA buffer at 25˚C for 1 h and then washed with 1X PBS and fixed with 4% paraformaldehyde at 25˚C for 15 min. Subsequently, the cells were permeabilized with 0.3% Triton X-100 at 25˚C for 15 min, followed by reacting with antibodies against LC3-B (0.5 μg/ml). Following incubation with Alexa Fluor® 488 goat anti-rabbit IgG (H+L) antibodies (1:500; cat. no. A21206, Invitrogen; Thermo Fisher Scientific Inc.) at 25˚C for 1 h, one drop ProLong™ Gold Antifade Mountant with DAPI (Thermo Fisher Scientific Inc.) was used to mount the coverslips at 25˚C for 1 min. The cells were observed under a ZEISS AXioskop2 fluorescence microscope (Carl Zeiss Microscopy, LLC).

Xenograft study. A total of 15 female athymic nude mice (5-weeks old; weight 15-17 g) were acquired from National Center for Experimental Animals of Taiwan and kept in

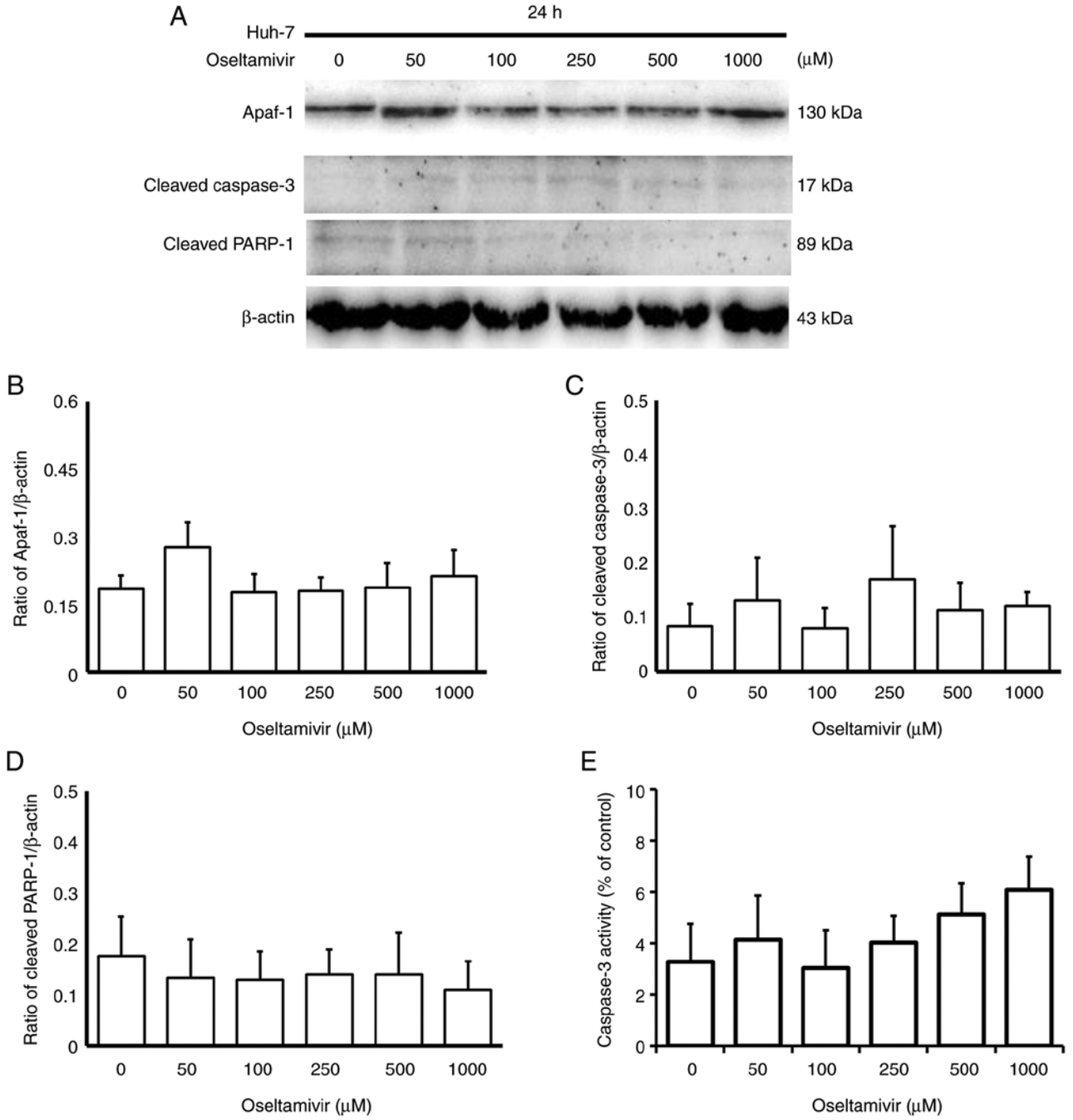

Figure 5. Effects of oseltamivir on apoptotic proteins and caspase-3 activity in Huh-7 cells. (A) Expression levels of Apaf-1, cleaved caspase-3 and cleaved PARP-1 in Huh-7 cells treated with oseltamivir for 24 h. Bars present the ratio of (B) Apaf-1, (C) cleaved caspase-3 and (D) cleaved PARP-1 with β-actin as the control. (E) Caspase-3 activity in Huh-7 cells treated with oseltamivir for 24 h. At least three-repeated tests were performed.

specific-pathogen-free (SPF) facilities with a 12-h light/dark cycle and a relative humidity in an airconditioned room of 55%. Animals were allowed free access to sterilized water and chow (Lab Diet 5001; PMI Nutrition International Inc.) at Chung Shan Medical University (Taichung, Taiwan). Study protocols were authorized by the Institutional Animal Care and Use Committee of Chung Shan Medical University, Taiwan, R.O.C. (IACUC approval no. 2542). The study was carried out in compliance with the ARRIVE guidelines (Animal Research: Reporting of *In Vivo* Experiments). A total of $5x10^6$ Huh-7 cells in PBS were hypodermically injected into the flank of mice at the age of 6-weeks old. The doses of oseltamivir used in the xenograft study were based on a previous study (16). When the tumor volumes reached ~100 mm^3, the mice were randomly divided into three groups including control, low dose- and high-dose groups and were daily intraperitoneally injected with PBS, 15 and 60 mg/kg oseltamivir, respectively. The tumor diameters and volume were measured every two days using a caliper. All the mice were sacrificed (performed on August 3, 2021) when the tumor volumes of the mice from the control group reached ~2,000 mm^3. Inhalation of carbon dioxide (CO_2) was used for mice euthanasia. The flow rate of CO_2 was 50% of the chamber volume/min. Following visual confirmation of respiratory

cessation of the mice, the CO_2 flow was maintained for 1 min to ensure the death of mice.

Statistical analysis. GraphPad Prism 5 software (GraphPad Software, Inc.) was used to calculate the significant differences among groups. For the MTT, wound healing, and Transwell migration assays, as well as ELISA and immunoblotting, two-way ANOVA with Bonferroni's post hoc test for multiple comparisons was performed to calculate the effects of drug treatment. $P<0.05$ was considered to indicate a statistically significant difference. All values are presented as the mean ± SEM.

Results

Effects of lamivudine, ribavirin and oseltamivir on the proliferation, migration and invasion of liver cancer cells. To assess the effects of antiviral drugs, including lamivudine, ribavirin, and oseltamivir, on liver cancer, Huh-7 and HepG2 cells were first treated with various concentrations of lamivudine, ribavirin, and oseltamivir. THLE-3 cells were used as normal control cells. Although lamivudine caused a statistically significant difference in cell viability compared with the control treatment (0 μM), lamivudine had little effect on the survival of THLE-3, Huh-7, and HepG2 cells (Fig. 1). All three cell lines exhibited significantly decreased viability in the presence of ribavirin and oseltamivir in a dose-dependent manner at 24 (Fig. 1A) and 48 h (Fig. 1B). Notably, Huh-7 and HepG2 cells exhibited significantly lower viability in the presence of 250 and 500 μM oseltamivir at 48 h compared with THLE-3 cells (Fig. 1B). Since more aggravated clinical adverse effects have been reported with ribavirin than oseltamivir, the following studies focused on the effects of oseltamivir on liver cancer cells. To further investigate the effects of oseltamivir on the migration and invasion of Huh-7 and HepG2 cells, wound healing and Transwell assays were performed. Significantly decreased migrating areas were detected in both Huh-7 and HepG2 cells treated with oseltamivir for 24 and 48 h (Figs. 2A and 3A). Significantly decreased migration and invasion were observed in both Huh-7 and HepG2 cells that were treated with oseltamivir for 24 h (Figs. 2B and 3B).

Oseltamivir induces autophagy but not apoptosis in Huh-7 cells. To verify whether apoptosis and autophagy are involved in oseltamivir-induced Huh-7 cell death, flow cytometry, immunoblotting, immunofluorescence, and caspase-3 ELISAs were performed. A slightly increased proportion of Huh-7 cells in the sub-G1 phase were observed following treatment with different concentrations of oseltamivir for 24 and 48 h (Fig. 4A-C). No statistically significant differences in the protein expression of Apaf-1, cleaved caspase-3 and cleaved PARP-1 (Fig. 5A-D) or the activity of caspase-3 (Fig. 5E) were observed in the presence of oseltamivir for 24 h. Notable protein expression of LC3-II was detected in Huh-7 cells treated with 250, 500, and 1,000 μM oseltamivir for 24 h (Fig. 6). In addition, a significantly higher ratio of LC3-II/LC3-I and increased protein expression of Beclin-1 was observed in Huh-7 cells in a dose-dependent manner (Fig. 7A and B). Conversely, significantly decreased protein expression of p62 was detected in Huh-7 cells treated with 250, 500, and 1,000 μM oseltamivir for 24 h (Fig. 7C).

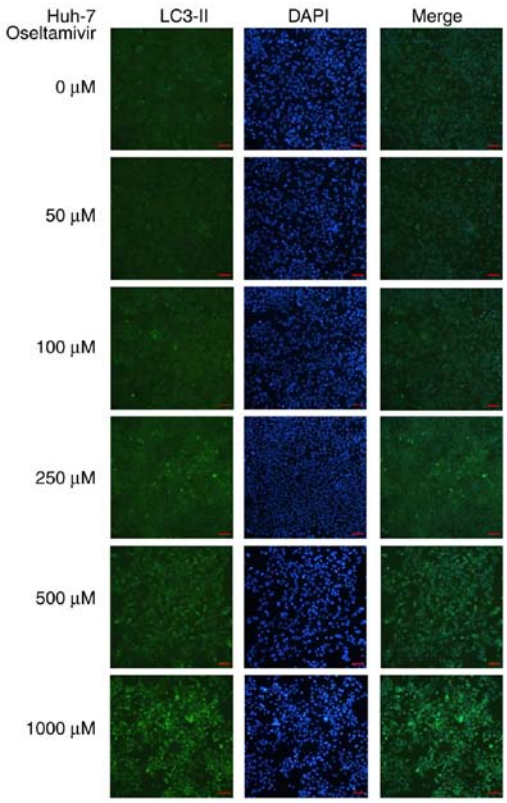

Figure 6. Effect of oseltamivir on inducing autophagy in Huh-7 cells. Representative images of immunofluorescence staining with LC3-II specific antibodies in Huh-7 cells in the presence of various concentrations of oseltamivir for 24 h. Scale bars, 5 μm.

Oseltamivir induces both apoptosis and autophagy in HepG2 cells. To verify whether apoptosis and autophagy are involved in oseltamivir-induced HepG2 cell death, flow cytometry, immunoblotting, immunofluorescence, and caspase-3 ELISAs were performed. Significantly increased proportion of HepG2 cells in the sub-G1 phase were observed following treatment with 500 and 1,000 μM oseltamivir for 24 h and with 100, 250, 500, and 1,000 μM for 48 h (Fig. 8A-C). Accordingly, significantly increased protein expression of Apaf-1, cleaved caspase-3, and cleaved PARP-1 was detected in HepG2 cells treated with oseltamivir for 24 h (Fig. 9A-D). Additionally, significantly increased caspase-3 activity was observed following treatment with 250, 500, and 1,000 μM oseltamivir for 24 h (Fig. 9E). A notably higher amount of LC3-II protein was observed in HepG2 cells treated with 250, 500, and 1,000 μM oseltamivir for 24 h (Fig. 10). A significantly higher ratio of LC3-II/LC3-I and increased protein expression of Beclin-1 were detected in Huh-7 cells in a dose-dependent manner, whereas significantly decreased protein expression of p62 was detected following treatment with 50, 100, 250, 500 and 1,000 μM oseltamivir for 24 h (Fig. 11). In addition, an autophagy inhibitor, CQ, was used to verify the participation of the autophagic mechanism to oseltamivir-induced death in Huh-7 and HepG2 cells (Fig. 12). Following pre-treatment of Huh-7 and HepG2 cells with CQ (25 μM) for 1 h, the cells were then incubated with 1 mM oseltamivir for 24 h. As anticipated, reduced p62 and increased

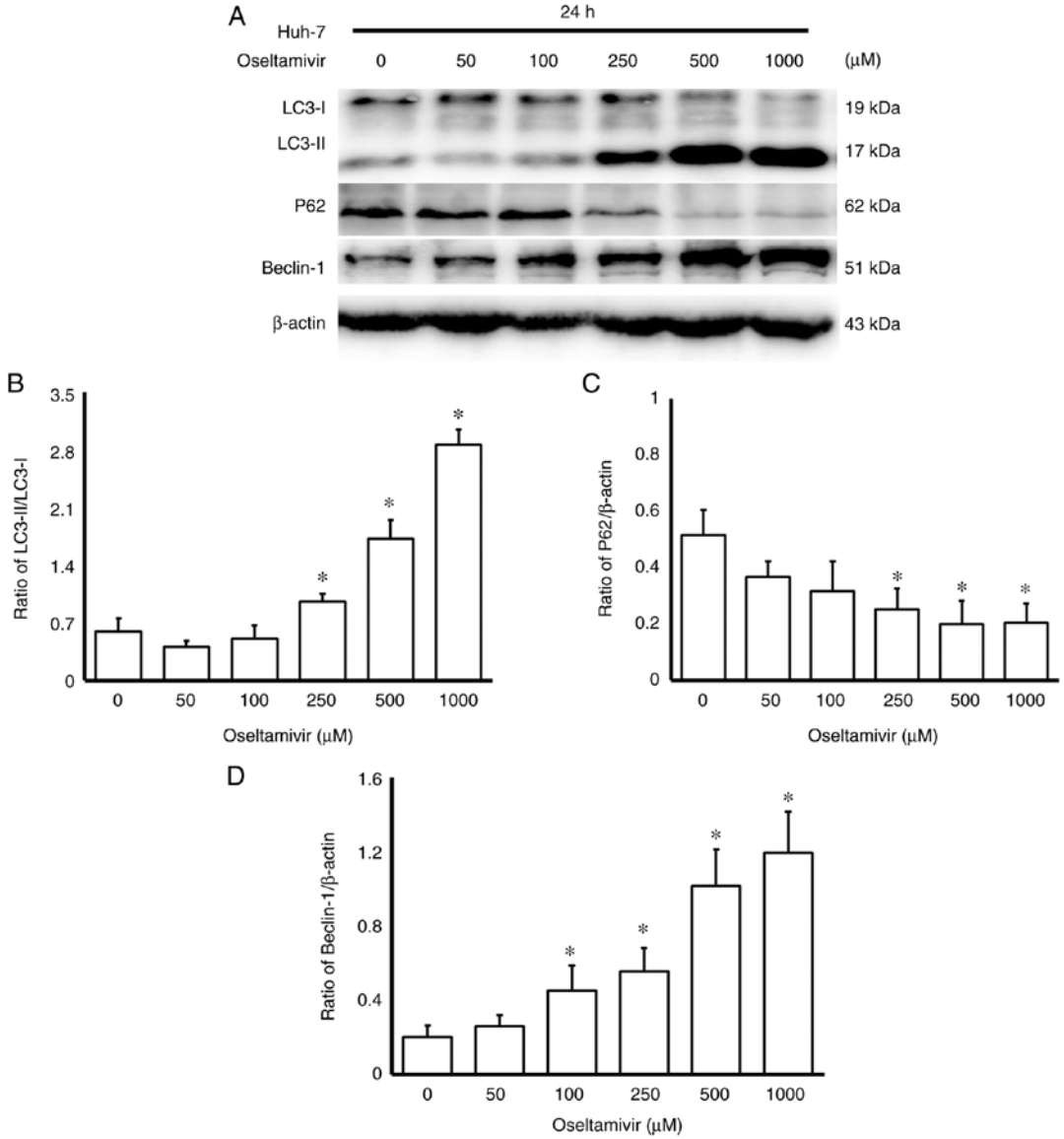

Figure 7. Effects of oseltamivir on autophagic proteins in Huh-7 cells. (A) Expression levels of LC3-II, LC3-I, p62 and Beclin-1 proteins in Huh-7 cells treated with oseltamivir for 24 h. Bars present the ratio of (B) LC3-II/LC3-I and the relative amount of (C) p62 and (D) Beclin-1 with β-actin as the control. At least three-repeated tests were performed. *P<0.05 compared with control (0 μM).

LC3-II protein levels were observed in both Huh-7 and HepG2 cells that were treated with 1 mM oseltamivir compared with the cells cultured in absence of both CQ and oseltamivir. Inhibition of lysosomal degradation by pre-treatment with CQ prevented the decomposition of LC3-II and p62 and resulted in accumulation of LC3-II and p62 (Fig. 12).

Oseltamivir inhibits the growth of xenografted Huh-7 cells in nude mice. To assess the effects of oseltamivir *in vivo*, xenografted tumors were generated by hypodermic injection of $5x10^6$ Huh-7 cells into athymic nude mice. When the tumor volume was ~100 mm^3, the animals were treated daily with PBS (control group), 15 mg/kg oseltamivir (low-dose group) and 60 mg/kg oseltamivir (high-dose group), respectively. A significantly smaller mean tumor volume was detected in the mice treated with 15 mg/kg or 60 mg/kg oseltamivir as compared with the mice treated with PBS from day-4 (Fig. 13A). Notably, a significantly smaller mean tumor volume was detected in the mice treated with 60 mg/kg oseltamivir as compared with the mice treated with 15 mg/kg from day-10 (Fig. 13A). Fig. 13B reveals the representative xenografted tumors retrieved at the end of the experiments.

Discussion

Since hepatitis virus infection has been strongly associated with the occurrence of liver cirrhosis and HCC, the traditional therapeutic strategy for liver cancer is to eliminate the hepatitis virus (7,17). In addition to drugs that target hepatitis viruses, various drugs against other viruses have been used for the treatment of liver cancer. However, information concerning the effects and related mechanisms of these antiviral drugs remains limited. In the present study, it was revealed that oseltamivir, an anti-influenza virus drug, significantly inhibited the growth and migration of Huh-7 and HepG2 cells. Oseltamivir also exerted differential effects on these liver

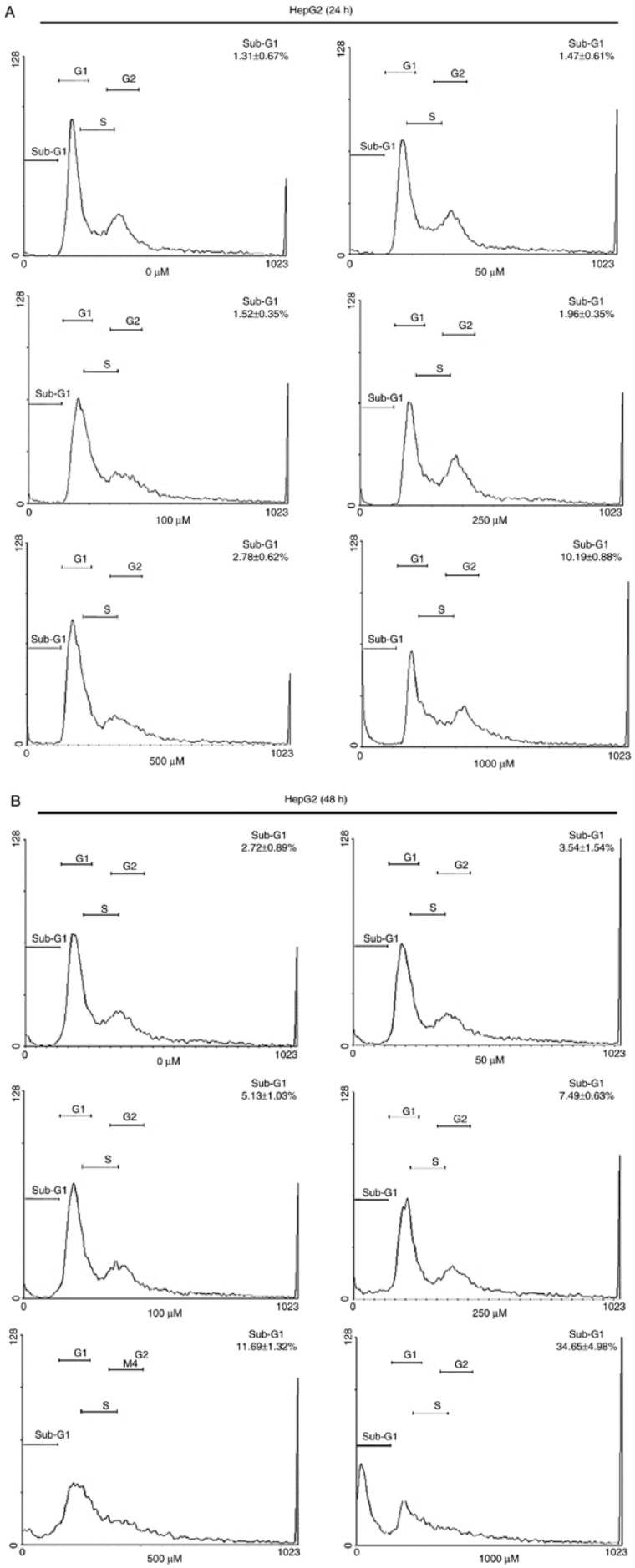

Figure 8. Continued.

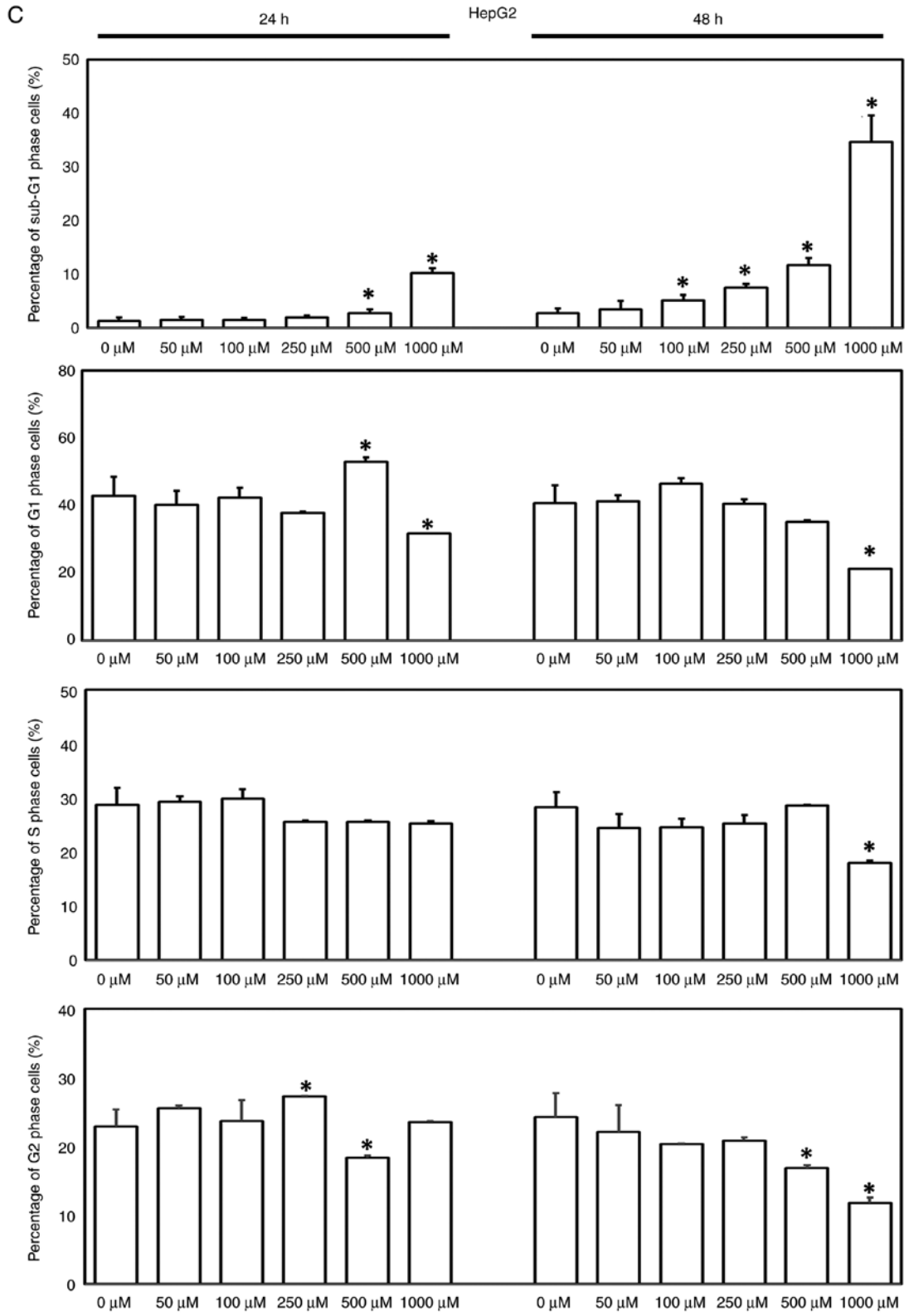

Figure 8. Effects of oseltamivir on the cell cycle in HepG2 cells. Representative results of flow cytometric analysis of HepG2 cells in the presence of oseltamivir for (A) 24 h and (B) 48 h. (C) Bar diagram showing the percentage of sub-G1, G1, S and G2 phases in HepG2 cells. At least three-repeated tests were performed. *P<0.05 compared with control (0 μM).

cancer cell lines by inducing apoptosis and autophagy alone or in combination.

Evidence has demonstrated dual roles of autophagy, namely, both tumor inhibitory and tumor promoting roles, in cancers. A variety of studies have revealed that autophagy promotes cancer cell death in early phases and survival in later phases (18-20). Autophagy may provide energy for excessive cancer cell proliferation or lead to the insufficient availability of nutrients for cancer cells by disrupting energy homeostasis, thus causing cell death (21). A previous study reported that

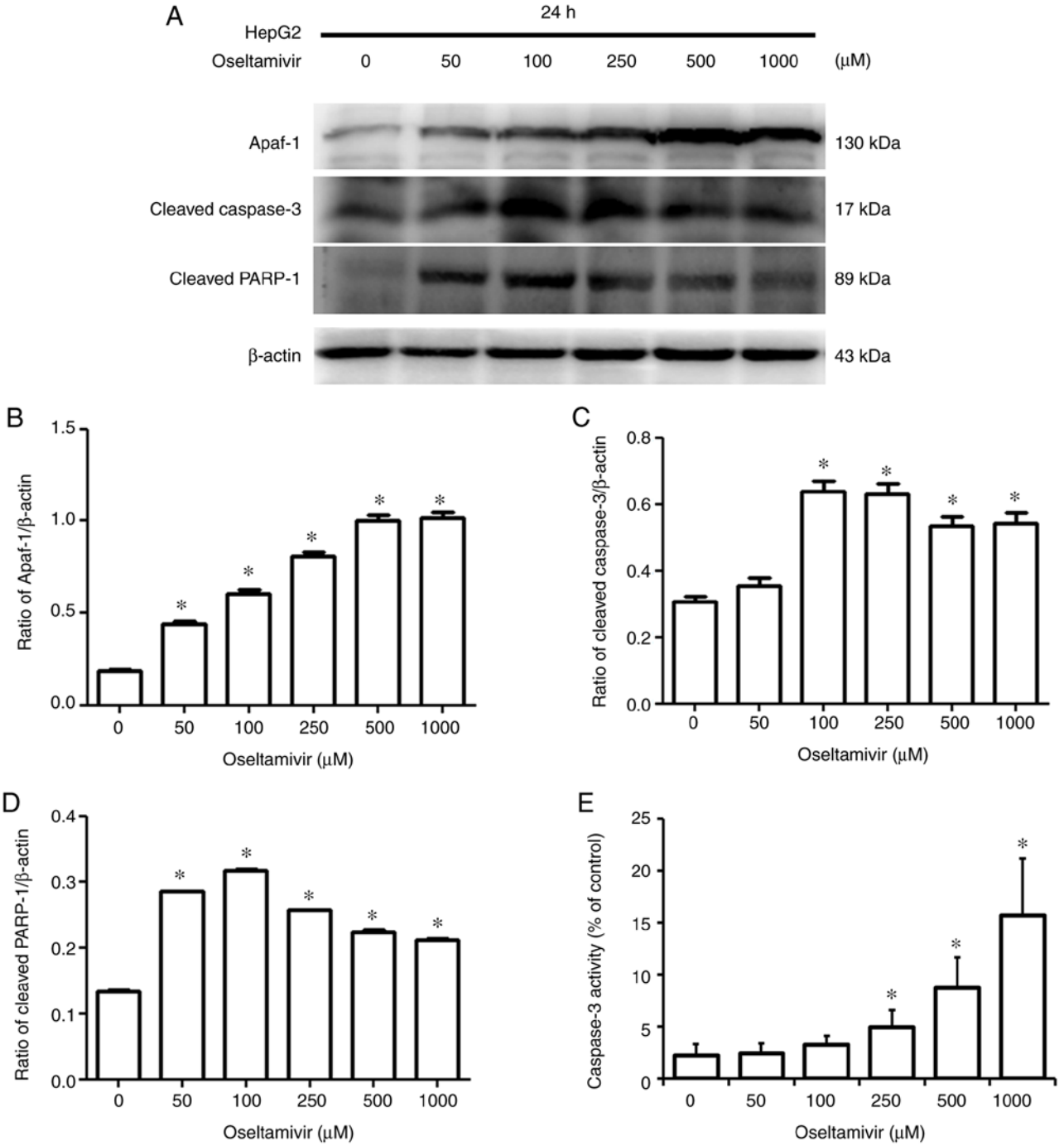

Figure 9. Effects of oseltamivir on apoptotic proteins and caspase-3 activity in HepG2 cells. (A) Expression levels of Apaf-1, cleaved caspase-3 and cleaved PARP-1 in HepG2 cells treated with oseltamivir for 24 h. Bars present the ratio of (B) Apaf-1, (C) cleaved caspase-3 and (D) cleaved PARP-1 with β-actin as the control. (E) Caspase-3 activity in HepG2 cells treated with oseltamivir for 24 h. At least three-repeated tests were performed. *P<0.05 compared with control (0 μM).

quinacrine-induced autophagy in ovarian cancer cells leads to excessive autophagic flux and promotes cell death (22). Another study indicated that dihydroartemisinin (DHA)-37, an analog of DHA, exhibits significant anticancer activity against A549 cells by triggering excessive autophagic cell death (23). A recent study also revealed that *Dendrobium officinale* polysaccharide significantly inhibits CT26 cell proliferation by inducing mitochondrial dysfunction and excessive autophagy (24). These findings suggested that excessive amounts of autophagy could be a potential strategy for causing cancer cell death. Accordingly, the present study reported, for the first time to the best of our knowledge, that oseltamivir induces excessive autophagic cell death in both Huh-7 cells and HepG2 cells, providing an alternative method for the treatment of liver cancer.

An alternative approach based on the use of non-oncological drugs for cancer treatment has attracted considerable attention in recent decades (25,26). Various types of non-oncological medicines, including antiviral drugs, have yielded promising *in vitro* results and are already being assessed in clinical

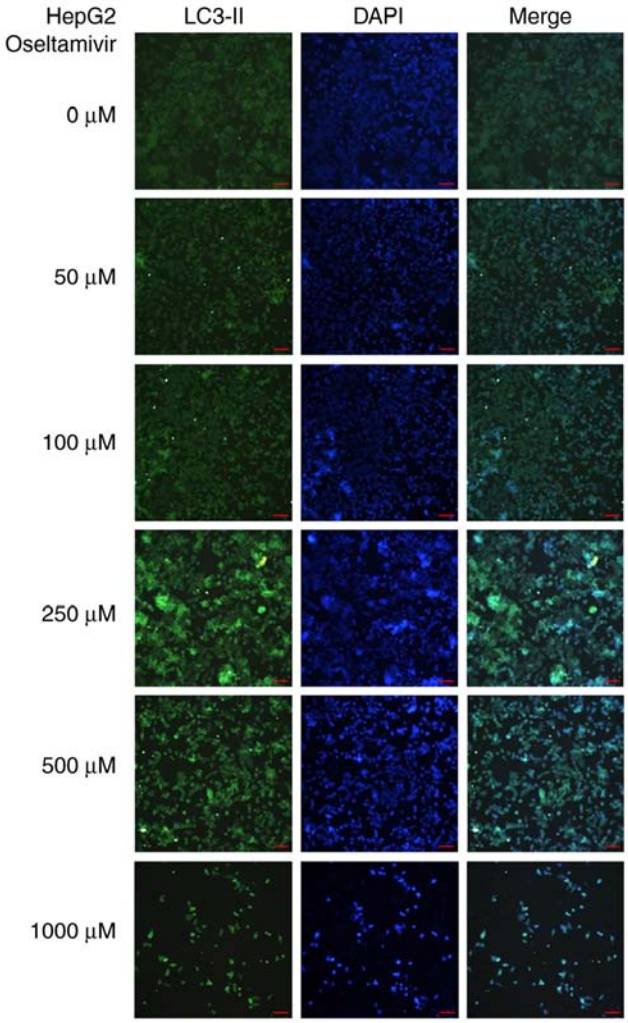

Figure 10. Effect of oseltamivir on inducing autophagy in HepG2 cells. Representative images of immunofluorescence staining with LC3-II specific antibodies in HepG2 cells in the presence of various concentrations of oseltamivir for 24 h. Scale bars, 5 μm.

trials (27). In the present study, it was revealed that antiviral drugs, including lamivudine, ribavirin, and oseltamivir, exerted significant inhibitory effects on the proliferation of Huh-7 and HepG2 cells. However, the concentrations of lamivudine required to inhibit the proliferation of these liver cancer cell lines were markedly higher than those of both ribavirin and oseltamivir. In addition, ribavirin usually needs to be combined with interferon in clinical treatment and requires a higher dose and longer treatment time, which lead to more serious side effects (28). Notably, the dose of oseltamivir that was significantly effective in inhibiting proliferation was markedly lower than that of ribavirin. Thus, the dose of this medication could be reduced while still achieving therapeutic efficacy, which could prevent adverse side effects, drug diversion, poisoning, and waste treatment (29). In addition to the significant inhibitory effects of oseltamivir on Huh-7 and HepG2 cells, these findings suggested additional potential of oseltamivir in the treatment of liver cancer in the clinic.

Therapeutic strategies targeting apoptosis (30,31) and autophagy (32,33) have long been used for cancer treatment. An interesting finding in the present study was the differential effects of oseltamivir on Huh-7 and HepG2 cells. Oseltamivir induced both autophagy and apoptosis in HepG2 cells but induced only autophagy in Huh-7 cells. This phenomenon may be attributed to the different characteristics of the two cell lines, particularly the mutation of p53 in Huh-7 cells (33). A previous genetic study reported that HepG2 cells have a N-ras mutation at codon 61, and Huh-7 cells have a missense mutation in the p53 gene at codon 220, resulting in an amino acid change of cysteine for tyrosine (34). p53 is one of the most well investigated and most frequently mutated genes in various human cancers (35). A previous study has indicated that the p53 gene plays an essential role in limiting cancer formation by modulating metabolism, reactive oxygen species production, and noncoding RNA expression and by enhancing autophagy or ferroptosis (36). Indeed, mutations in the p53 gene have been demonstrated to be involved in cancer formation and progression and are present in ~50% of aggressive tumors (35). Notably, two clinical studies indicated that the presence of missense p53 mutations is significantly associated with breast cancer specificity and overall mortality (37,38). Interestingly, p53 was also found to play a key role on controlling the switch between autophagy and apoptosis. An *in vitro* model reported that sodium selenite switched protective autophagy to apoptosis in both a p53-wild type (NB4 cells) and p53-mutant cell model (Jurkat cells) (39,40). These findings may provide possible explanations of the difference

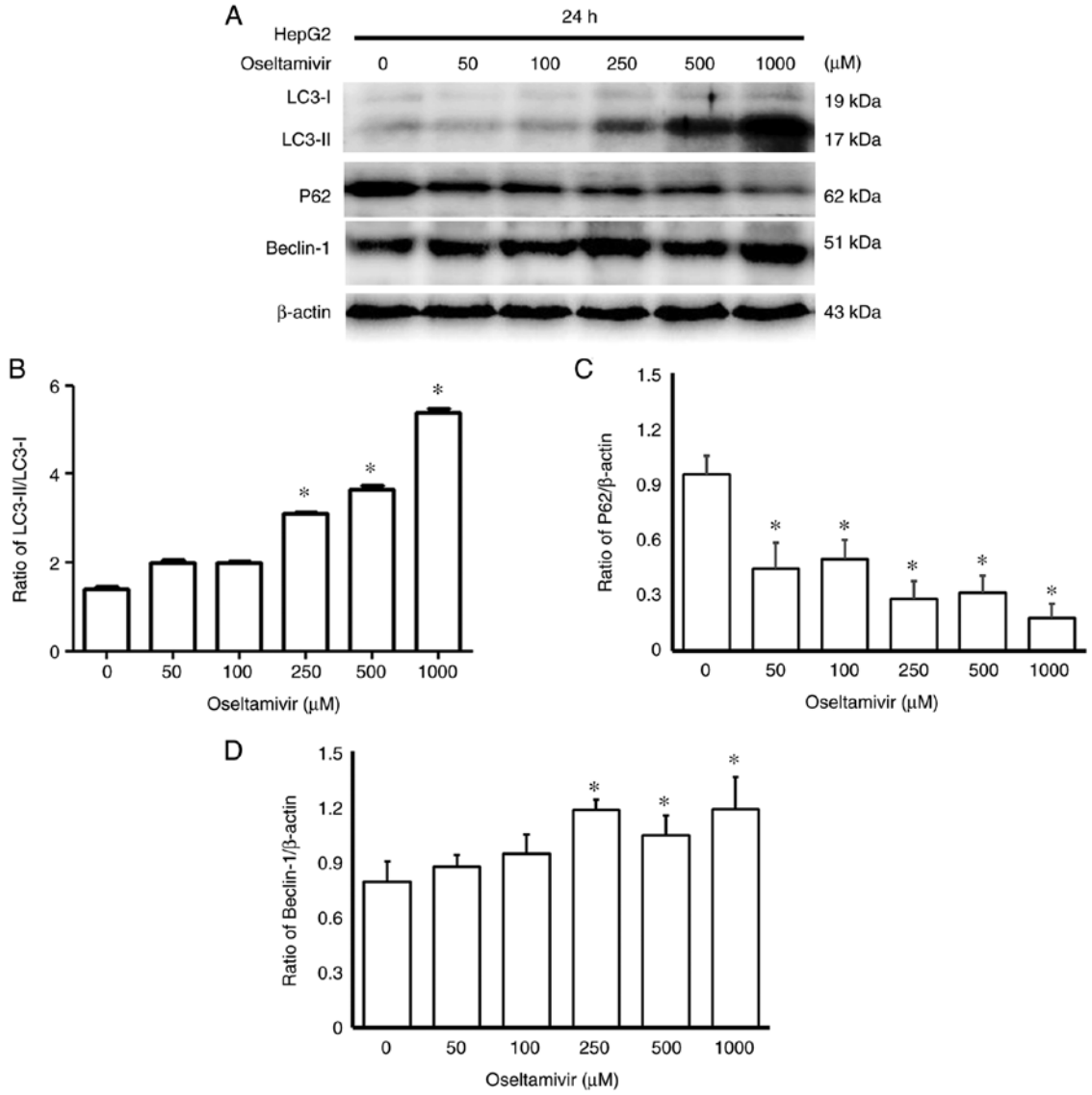

Figure 11. Effects of oseltamivir on autophagic proteins in HepG2 cells. (A) Expression levels of LC3-II, LC3-I, p62 and Beclin-1 proteins in HepG2 cells treated with oseltamivir for 24 h. Bars present the ratio of (B) LC3-II/LC3-I and the relative amount of (C) p62 and (D) Beclin-1 with β-actin as the control. At least three-repeated tests were performed. *P<0.05 compared with control (0 μM).

in oseltamivir-induced death between Huh-7 and HepG2 cells. However, further investigations such as xenografted HepG2 experiments and underlying signaling analysis are required to identify the precise mechanism of oseltamivir-induced cell apoptosis and/or autophagy in Huh-7 and HepG2 cells.

In addition, the role of p62 in autophagy and apoptosis has received a great amount of attention in recent years. The scaffold protein p62, namely sequestosome 1 (SQSTM1), is well-known as a critical regulator in the autophagic process by directly binding LC3 for autophagosome generation (41,42). Evidence has indicated that p62/SQSTM1 mediated a variety of essential cellular processes, including autophagy and apoptosis, through its different domains (42,43). In fact, studies have demonstrated that p62 binds LC3 by the LC3-interacting region (LIR) within p62 and promotes the formation of autophagosomes (44,45). Additionally, p62 has also been reported to induce apoptosis through the caspase-8 activation at the autophagosomal membrane (46). In the presence of culin3, caspase-8 was modified and interacted with p62 and TRAF6, which leads to the activation of caspase-8 downstream caspase and apoptosis (47,48). These findings indicated a dual role of p62 in autophagy and apoptosis and may provide another possible rationale for explaining the difference of oseltamivir-induced autophagy/apoptosis in Huh-7 and HepG2 cells. Definitely, further experiments are merited to investigate the precise role of p62 on oseltamivir-induced cell death in Huh-7 and HepG2 cells.

Neuraminidase (NEU) is the enzyme expressed on the surface of influenza viruses, and it facilitates the release and trafficking of influenza viruses within the respiratory tract (39). Oseltamivir (Tamiflu) is an FDA-approved NEU inhibitor for the prevention and treatment of influenza A and B infections (49,50). Certain investigations have been conducted on the alternative use of oseltamivir in cancer treatment. A previous study on alternative treatments for pancreatic cancer indicated that oseltamivir inhibits the activity of NEU-1 (Sialidase) and suppresses intrinsic signaling that promotes human pancreatic cancer (PANC1) cell survival (51). In addition, oseltamivir also overcame the chemoresistance of PANC1 cells to cisplatin and

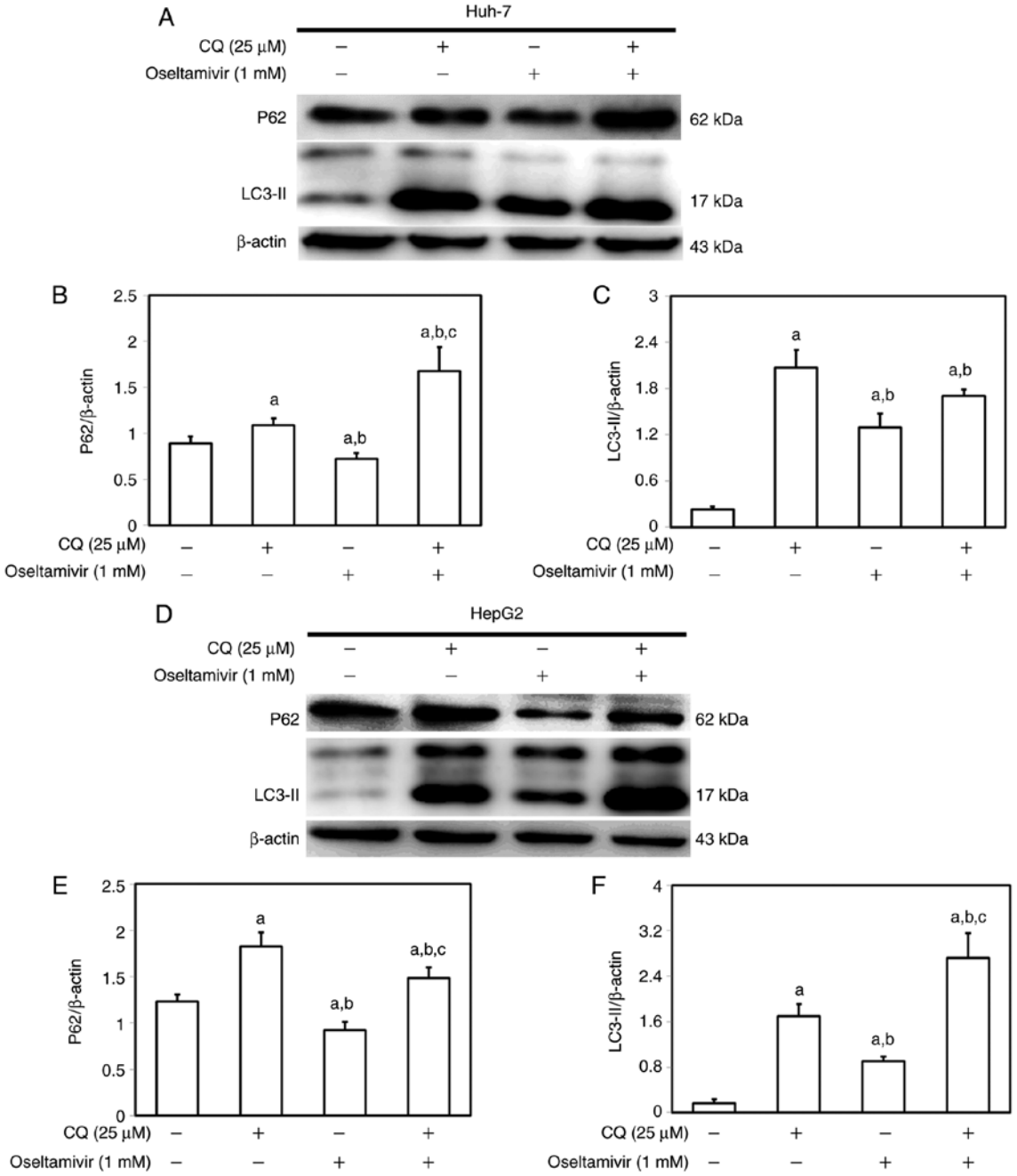

Figure 12. Involvement of autophagy in the response of Huh-7 and HepG2 cells treated with oseltamivir. Huh7 and HepG2 cells were pre-treated with 25 μM CQ for 1 h prior to oseltamivir treatment (1 mM). (A and D) Cell lysates were harvested following 24 h and p62 and LC3-II proteins were detected by western blotting. Bars represent protein quantification of (B and E) p62 and (C and F) LC3-II relative to β-actin. Similar results were observed in 3 repeated experiments. [a]P<0.05 compared with the control group; [b]P<0.05 compared with the CQ (25 μM) group; and [c]P<0.05 compared with the oseltamivir (1 mM) group. CQ, chloroquine.

gemcitabine alone or in combination by reversing changes in E-cadherin and N-cadherin expression (41). A recent study indicated an association between NEU-1 and HCC (51). Notably increased mRNA and protein expression of NEU-1 was observed in HBV-related HCC tissues, and this increased expression was caused by the binding of the HBV core protein to NF-KB on the NEU-1 promoter, which led to downstream oncogenic signaling and epithelial-mesenchymal transition (EMT) in HCC cells, including Huh-7 and HepG2 cells (52). These findings indicated the involvement of NEU in the carcinogenesis of HCC. Consistently, the present study was the first to report the anti-liver cancer activity of oseltamivir by inducing apoptosis in Huh-7 cells and inducing both apoptosis and autophagy in HepG2 cells. However, the roles of NEU and intrinsic signaling in oseltamivir-induced Huh-7 and HepG2 cell death remain unknown and warrant further investigation in order to elucidate the precise mechanism underlying the oseltamivir-induced cell death of Huh-7 and HepG2 cells. In summary, the present study provided novel findings about the use of non-oncological drugs for the treatment of liver cancer and suggests the use of oseltamivir as an alternative approach for liver cancer treatment.

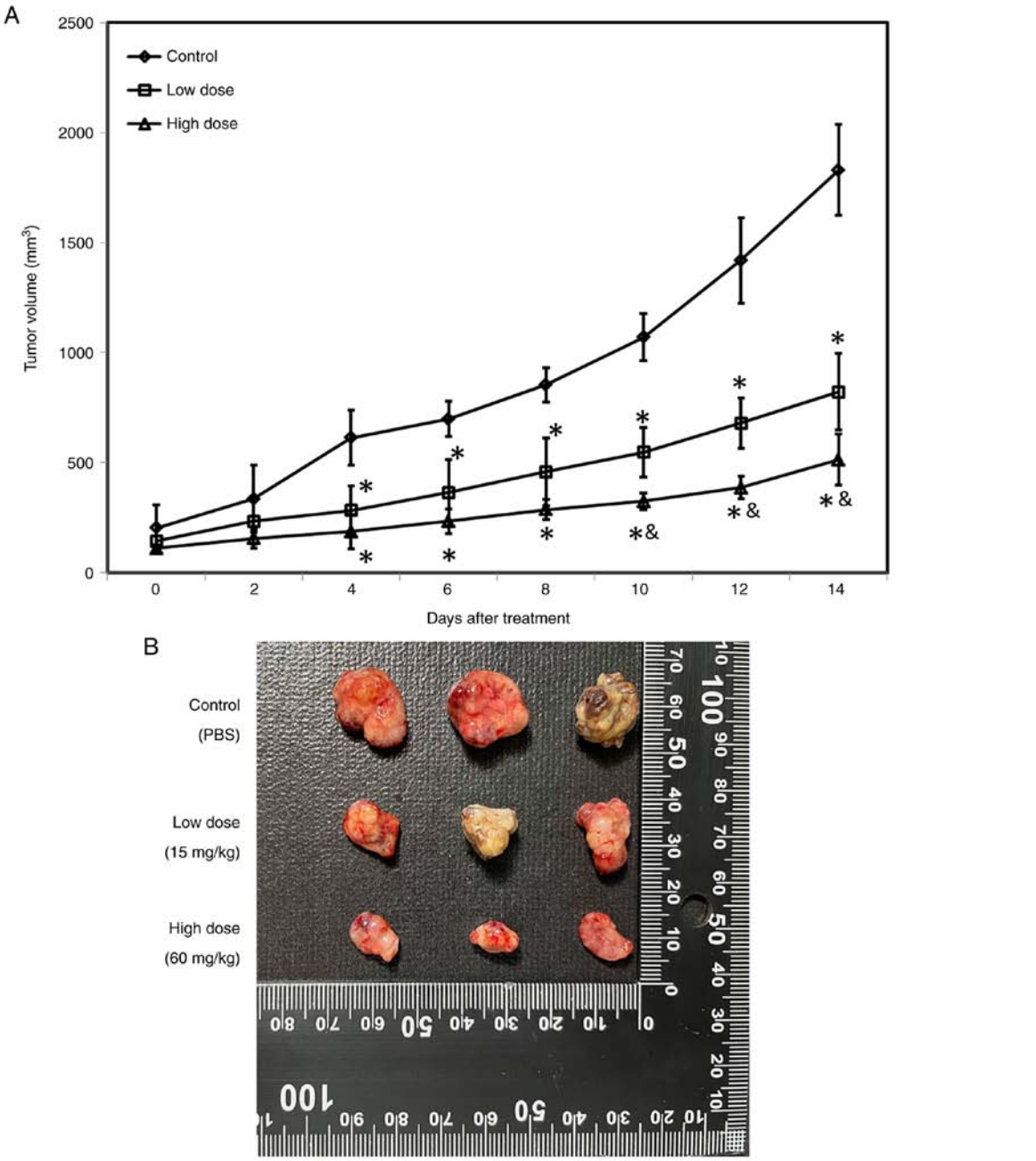

Figure 13. Effects of oseltamivir on xenografted Huh-7 cells in athymic nude mice. (A) The mice were divided into three groups (n=5) and were intraperitoneally injected with PBS (control group), 15 mg/kg oseltamivir (low-dose group) and 60 mg/kg oseltamivir (high-dose group), respectively. (B) Representative images of the excised xenograft tumors from the different groups of mice. *P<0.05 compared with the control group; and &P<0.05 compared with the low-dose group.

Acknowledgements

Not applicable.

Funding

The present study was funded by Chung Shan Medical University and Changhua Christian Hospital (grant no. CSMU-CCH-109-05), and the experimental supplies in the cell study were partially supported by the Ministry of Science and Technology, Taiwan, R.O.C. (grant no. MOST-109-2314-B040-021). The funders had no role in the study design, data collection and analysis, decision to publish, or preparation of the manuscript.

Availability of data and materials

All data generated or analyzed during this study are included in this published article.

Authors' contributions

PJH and CCC were involved in the study conception and design. MHH and JLY performed experiments and analysis of data. TCH was involved in the study conception and design, drafting and revising of the manuscript, performing experiments, analysis of data, and study supervision. BST was involved in the study conception and design, drafting and

revising of the manuscript, and analysis of data. BST and TCH confirm the authenticity of all the raw data. All authors read and approved the final manuscript.

Ethics approval and consent to participate

Animal experiments were performed in accordance with the principles of replacement, refinement and reduction and were approved (approval no. 2542) by the Institutional Animal Care and Use Committee (IACUC) of Chung Shan Medical University (Taichung, Taiwan, R.O.C.).

Patient consent for publication

Not applicable.

Competing interests

The authors declare that they have no competing interests.

References

1. Llovet JM, Zucman-Rossi J, Pikarsky E, Sangro B, Schwartz M, Sherman M and Gores G: Hepatocellular carcinoma. Nat Rev Dis Primers 14: 16018, 2016.
2. Forner A, Reig M and Bruix J: Hepatocellular carcinoma. The Lancet 391: 1301-1314, 2018.
3. Kuo CN, Liao YM, Kuo LN, Tsai HJ, Chang WC and Yen Y: Cancers in Taiwan: Practical insight from epidemiology, treatments, biomarkers, and cost. J Formos Med Assoc 119: 1731-1741, 2020.
4. Polesel J, Zucchetto A, Montella M, Dal Maso L, Crispo A, La Vecchia C, Serraino D, Franceschi S and Talamini R: The impact of obesity and diabetes mellitus on the risk of hepatocellular carcinoma. Ann Oncol 20: 353-357, 2009.
5. Li S, Saviano A, Erstad DJ, Hoshida Y, Fuchs BC, Baumert T and Tanabe KK: Risk factors, pathogenesis, and strategies for hepatocellular carcinoma prevention: Emphasis on secondary prevention and its translational challenges. J Clin Med 9: 3817, 2020.
6. Bosch FX, Ribes J, Cléries R and Díaz M: Epidemiology of hepatocellular carcinoma. Clin Liver Dis 9: 191-211, 2005.
7. Dash S, Aydin Y, Widmer KE and Nayak L: Hepatocellular carcinoma mechanisms associated with chronic HCV infection and the impact of direct-acting antiviral treatment. J Hepatocell Carcinoma 7: 45-76, 2020.
8. Sung PS and Shin EC: Immunological mechanisms for hepatocellular carcinoma risk after direct-acting antiviral treatment of hepatitis C virus infection. J Clin Med 10: 221, 2021.
9. Andrisani O: Epigenetic mechanisms in hepatitis B virus-associated hepatocellular carcinoma. Hepatoma Res 7: 12, 2021.
10. Ulcickas Yood M, Quesenberry Jr CP, Guo D, Wells K, Shan J, Sanders L, Skovron ML, Iloeje U, Caldwell C and Manos MM: Incidence of hepatocellular carcinoma among individuals with heaptitis B virus infection identified using an automated data algorithm. J Viral Hepat 15: 28-36, 2008.
11. Fattovich G, Stroffolini T, Zagni I and Donato F: Hepatocellular carcinoma in cirrhosis: Incidence and risk factors. Gastroenterology 127 (5 Suppl 1): S35-S50, 2004.
12. Nguyen VT, Law MG and Dore GJ: Hepatitis B-related hepatocellular carcinoma: Epidemiological characteristics and disease burden. J Viral Hepat 16: 453-463, 2009.
13. Kim GA, Lim YS, Han S, Choi J, Shim JH, Kim KM, Lee HC and Lee YS: High risk of hepatocellular carcinoma and death in patients with immune-tolerant-phase chronic hepatitis B. Gut 67: 945-952, 2018.
14. Pons F, Varela M and Llovet JM: Staging systems in hepatocellular carcinoma. HPB (Oxford) 7: 35-41, 2005.
15. Mak LY, Cruz-Ramón V, Chinchilla-López P, Torres HA, LoConte NK, Rice JP, Foxhall LE, Sturgis EM, Merrill JK, Bailey HH, *et al*: Global epidemiology, prevention, and management of hepatocellular carcinoma. Am Soc Clin Oncol Educ Book 38: 262-279, 2018.
16. Haxho F, Allison S, Alghamdi F, Brodhagen L, Kuta VE, Abdulkhalek S, Neufeld RJ and Szewczuk MR: Oseltamivir phosphate monotherapy ablates tumor neovascularization, growth, and metastasis in mouse model of human triple-negative breast adenocarcinoma. Breast Cancer (Dove Med Press) 6: 191-203, 2014.
17. Xu HZ, Liu YP, Guleng B and Ren JL: Hepatitis B virus-related hepatocellular carcinoma: Pathogenic mechanisms and novel therapeutic interventions. Gastrointest Tumors 1: 135-145, 2014.
18. Levy JM and Thorburn A: Targeting autophagy during cancer therapy to improve clinical outcomes. Pharmacol Ther 131: 130-141, 2011.
19. Chen C, Gao H and Su X: Autophagy-related signaling pathways are involved in cancer (Review). Exp Ther Med 22: 710, 2021.
20. Lee XC, Werner E and Falasca M: Molecular mechanism of autophagy and its regulation by cannabinoids in cancer. Cancers (Basel) 13: 1211, 2021.
21. Islam Khan MZ and Law HK: Cancer Susceptibility Candidate 9 (CASC9) promotes colorectal cancer carcinogenesis via mTOR-dependent autophagy and epithelial-mesenchymal transition pathways. Front Mol Biosci 8: 627022, 2021.
22. Khurana A, Roy D, Kalogera E, Mondal S, Wen X, He X, Dowdy S and Shridhar V: Quinacrine promotes autophagic cell death and chemosensitivity in ovarian cancer and attenuates tumor growth. Oncotarget 6: 36354-36369, 2015.
23. Liu X, Wu J, Fan M, Shen C, Dai W, Bao Y, Liu JH and Yu BY: Novel dihydroartemisinin derivative DHA-37 induces autophagic cell death through upregulation of HMGB1 in A549 cells. Cell Death Dis 9: 1048, 2018.
24. Zhang K, Zhou X, Wang J, Zhou Y, Qi W, Chen H, Nie S and Xie M: Dendrobium officinale polysaccharide triggers mitochondrial disorder to induce colon cancer cell death via ROS-AMPK-autophagy pathway. Carbohydr Polym 264: 118018, 2021.
25. Armando RG, Mengual Gómez DL and Gomez DE: New drugs are not enough-drug repositioning in oncology: An update. Int J Oncol 56: 651-684, 2020.
26. Nunes M, Henriques Abreu M, Bartosch C and Ricardo S: Recycling the purpose of old drugs to treat ovarian cancer. Int J Mol Sci 21: 7768, 2020.
27. Hampson L, Maranga IO, Masinde MS, Oliver AW, Batman G, He X, Desai M, Okemwa PM, Stringfellow H, Martin-Hirsch P, *et al*: A single-arm, proof-of-concept trial of Lopimune (Lopinavir/Ritonavir) as a treatment for HPV-related pre-invasive cervical disease. PLoS One 11: e0147917, 2016.
28. Beaucourt S and Vignuzzi M: Ribavirin: A drug active against many viruses with multiple effects on virus replication and propagation. Molecular basis of ribavirin resistance. Curr Opin Virol 8: 10-15, 2014.
29. Daughton CG and Ruhoy IS: Lower-dose prescribing: Minimizing 'side effects' of pharmaceuticals on society and the environment. Sci Total Environ 443: 324-337, 2013.
30. von Karstedt S, Montinaro A and Walczak H: Exploring the TRAILs less travelled: TRAIL in cancer biology and therapy. Nat Rev Cancer 17: 352-366, 2017.
31. Tan S, Liu X, Chen L, Wu X, Tao L, Pan X, Tan S, Liu H, Jiang J and Wu B: Fas/FasL mediates NF-kappaBp65/PUMA-modulated hepatocytes apoptosis via autophagy to drive liver fibrosis. Cell Death Dis 12: 474, 2021.
32. Alvarez-Meythaler JG, Garcia-Mayea Y, Mir C, Kondoh H and LLeonart ME: Autophagy takes center stage as a possible cancer hallmark. Front Oncol 10: 586069, 2020.
33. Buzun K, Gornowicz A, Lesyk R, Bielawski K and Bielawska A: Autophagy modulators in cancer therapy. Int J Mol Sci 22: 5804, 2021.
34. Hsu IC, Tokiwa T, Bennett W, Metcalf RA, Welsh JA, Sun T and Harris CC: p53 gene mutation and integrated hepatitis B viral DNA sequences in human liver cancer cell lines. Carcinogenesis 14: 987-992, 1993.
35. Duffy MJ, Synnott NC and Crown J: Mutant p53 as a target for cancer treatment. Eur J Cancer 83: 258-265, 2017.
36. Braithwaite AW, Royds JA and Jackson P: The p53 story: Layers of complexity. Carcinogenesis 26: 1161-1169, 2005.
37. Berns EM, van Staveren IL, Look MP, Smid M, Klijn JG and Foekens JA: Mutations in residues of TP53 that directly contact DNA predict poor outcome in human primary breast cancer. Br J Cancer 77: 1130-1136, 1998.
38. Rossner P Jr, Gammon MD, Zhang YJ, Terry MB, Hibshoosh H, Memeo L, Mansukhani M, Long CM, Garbowski G, Agrawal M, *et al*: Mutations in p53, p53 protein overexpression and breast cancer survival. J Cell Mol Med 13: 3847-3857, 2009.

39. Guo JY and White E: Autophagy, metabolism, and cancer. Cold Spring Harb Symp Quant Biol 81: 73-78, 2016.
40. Shi K, An J, Qian K, Zhao X, Li F, Ma X, Wang Y and Zhang Y: p53 controls the switch between autophagy and apoptosis through regulation of PLSCR1 in sodium selenite-treated leukemia cells. Exp Cell Res 389: 111879, 2020.
41. Itakura E and Mizushima N: p62 Targeting to the autophagosome formation site requires self-oligomerization but not LC3 binding. J Cell Biol 192: 17-27, 2011.
42. Islam MA, Sooro MA and Zhang P: Autophagic Regulation of p62 is critical for cancer therapy. Int J Mol Sci 19: 1405, 2018.
43. Moscat J, Diaz-Meco MT and Wooten MW: Signal integration and diversification through the p62 scaffold protein. Trends Biochem Sci 32: 95-100, 2007.
44. Ichimura Y, Kominami E, Tanaka K and Komatsu M: Selective turnover of p62/A170/SQSTM1 by autophagy. Autophagy 4: 1063-1066, 2008.
45. Lin X, Li S, Zhao Y, Ma X, Zhang K, He X and Wang Z: Interaction domains of p62: A bridge between p62 and selective autophagy. DNA Cell Biol 32: 220-227, 2013.
46. Young MM, Takahashi Y, Khan O, Park S, Hori T, Yun J, Sharma AK, Amin S, Hu CD and Zhang J: Autophagosomal membrane serves as platform for intracellular death-inducing signaling complex (iDISC)-mediated caspase-8 activation and apoptosis. J Biol Chem 287: 12455-12468, 2012.
47. Sanz L, Diaz-Meco MT, Nakano H and Moscat J: The atypical PKC-interacting protein p62 channels NF-kappaB activation by the IL-1-TRAF6 pathway. EMBO J 19: 1576-1586, 2000.
48. Jin Z, Li Y, Pitti R, Lawrence D, Pham VC, Lill JR and Ashkenazi A: Cullin3-based polyubiquitination and p62-dependent aggregation of caspase-8 mediate extrinsic apoptosis signaling. Cell 137: 721-735, 2009.
49. Cooper NJ, Sutton AJ, Abrams KR, Wailoo A, Turner D and Nicholson KG: Effectiveness of neuraminidase inhibitors in treatment and prevention of influenza A and B: Systematic review and meta-analyses of randomised controlled trials. BMJ 326: 1235, 2003.
50. Hayden FG, Treanor JJ, Fritz RS, Lobo M, Betts RF, Miller M, Kinnersley N, Mills RG, Ward P and Straus SE: Use of the oral neuraminidase inhibitor oseltamivir in experimental human influenza: Randomized controlled trials for prevention and treatment. JAMA 282: 1240-1246, 1999.
51. O'Shea LK, Abdulkhalek S, Allison S, Neufeld RJ and Szewczuk MR: Therapeutic targeting of Neu1 sialidase with oseltamivir phosphate (Tamiflu) disables cancer cell survival in human pancreatic cancer with acquired chemoresistance. Onco Targets Ther 7: 117-134, 2014.
52. Kong F, Li N, Tu T, Tao Y, Bi Y, Yuan D, Zhang N, Yang X, Kong D, You H, *et al*: Hepatitis B virus core protein promotes the expression of neuraminidase 1 to facilitate hepatocarcinogenesis. Lab Invest 100: 1602-1617, 2020.